ACS APPLIED MATERIALS & INTERFACES
Research Article
www.acsami.org

Alucone Interlayers to Minimize Stress Caused by Thermal Expansion Mismatch between Al_2O_3 Films and Teflon Substrates

Shih-Hui Jen[†] and Steven M. George*[,†,‡]

[†]Department of Chemistry and Biochemistry and [‡]Department of Chemical and Biological Engineering, University of Colorado, Boulder, Colorado 80309, United States

Robert S. McLean and Peter F. Carcia

DuPont Central Research & Development, Wilmington, Delaware 19803, United States

ABSTRACT: Alucone films were employed as interlayers to minimize stress caused by thermal expansion mismatch between Al_2O_3 films grown by atomic layer deposition (ALD) and Teflon fluorinated ethylene propylene (FEP) substrates. The alucone films were grown by molecular layer deposition (MLD) using trimethylaluminum (TMA), ethylene glycol (EG), and H_2O. Without the alucone interlayer, the Al_2O_3 films were susceptible to cracking resulting from the high coefficient of thermal expansion (CTE) mismatch between the Al_2O_3 film and the Teflon FEP substrate. Cracking was observed by field emission scanning electron microscopy (FE-SEM) images of Al_2O_3 films grown directly on Teflon FEP substrates at temperatures from 100 to 160 °C and then cooled to room temperature. With an alucone interlayer, the Al_2O_3 film had a crack density that was reduced progressively versus alucone interlayer thickness. For Al_2O_3 film thicknesses of 48 nm deposited at 135 °C, no cracks were observed for alucone interlayer thicknesses >60 nm on 50 μm thick Teflon FEP substrates. For thinner Al_2O_3 film thicknesses of 21 nm deposited at 135 °C, no cracks were observed for alucone interlayer thicknesses >40 nm on 50 μm thick Teflon FEP substrates. Slightly higher alucone interlayer thicknesses were required to prevent cracking on thicker Teflon FEP substrates with a thickness of 125 μm. The alucone interlayer linearly reduced the compressive stress on the Al_2O_3 film caused by the thermal expansion mismatch between the Al_2O_3 coating and the Teflon FEP substrate. The average compressive stress reduction per thickness of the alucone interlayer was determined to be 8.5 ± 2.3 MPa/nm. Comparison of critical tensile strains for alucone films on Teflon FEP and HSPEN substrates revealed that residual compressive stress in the alucone film on Teflon FEP could help offset applied tensile stress and lead to the attainment of much higher critical tensile strains.

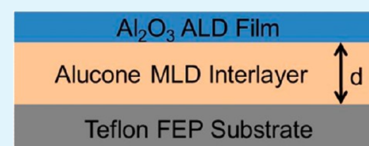

KEYWORDS: *thermal stress, Al_2O_3, Teflon, atomic layer deposition, molecular layer deposition, alucone*

I. INTRODUCTION

Al_2O_3 coatings grown by atomic layer deposition (ALD) are excellent gas diffusion barriers on polymers.[1−3] Recent measurements of the water vapor transmission rate (WVTR) for Al_2O_3 ALD on polyethylene naphthalate (PEN) at 38 °C/85% RH using the Ca test have yielded an upper limit for the WVTR of ~5×10^{-5} g/m^2/day for Al_2O_3 film thicknesses of ≥10 nm.[1] The WVTR is an upper limit because the Al_2O_3 ALD barriers give equivalent performance to the glass lid controls.[1] These small WVTR values are important as gas diffusion barriers for organic light-emitting diodes (OLEDs) or thin film photovoltaic devices.[4−6]

One problem facing Al_2O_3 ALD barriers on polymer substrates is the mismatch between the coefficient of thermal expansion (CTE) of the polymer substrate and the Al_2O_3 coating.[7,8] This problem is particularly severe for Al_2O_3 barriers on fluoropolymers, such as Teflon FEP, that have large CTEs.[9] Teflon FEP and other fluoropolymer substrates are important for thin film solar devices because of their ability to withstand outdoor conditions in the sun without degradation.[7]

Our earlier studies demonstrated that the thermal expansion mismatch between the Al_2O_3 ALD film and the Teflon FEP substrate could lead to film cracking resulting from compressive strain upon cooling after Al_2O_3 ALD at 100−160 °C.[8] The critical compressive strain was determined by characterizing the cracks in the Al_2O_3 film versus compressive strain. The compressive stress on the Al_2O_3 films could be varied by changing the temperature difference, ΔT, between the deposition temperature and room temperature.[8] The measurements revealed that the threshold compressive strain for cracking is higher for the thinner Al_2O_3 coatings.[8] Measurements of cracking versus tensile strain also revealed that the critical tensile strains were higher for thinner Al_2O_3 coatings.[8]

Interlayer materials are needed at the interface between the Al_2O_3 film and the underlying Teflon FEP substrate to minimize the compressive stress caused by CTE mismatch. The interlayer is a compensating compliant layer that can reduce the stress caused by CTE mismatch.[10] The interlayer can have an intermediate value for the CTE between the deposited film and the underlying substrate. The interlayer can

Received: December 12, 2012
Accepted: December 28, 2012
Published: December 28, 2012

 © 2012 American Chemical Society

also be a functionally graded material that makes a continuous transition between the low CTE of the film to the high CTE of the underlying substrate. Calculations have been performed that evaluate various interlayer geometries and suggest interlayer architectures that produce the lowest residual stress and minimize the CTE mismatch.[11,12]

In this study, an alucone interlayer grown by molecular layer deposition (MLD) was used as a compliant interlayer to reduce the stress applied on the Al_2O_3 film by the Teflon FEP substrate resulting from thermal expansion mismatch. The cracking density in the Al_2O_3 ALD film was examined versus the thickness of the alucone interlayer. The alucone interlayer was able to eliminate the cracking of the Al_2O_3 film. Smaller thicknesses of the alucone interlayer were required to prevent the cracking of the Al_2O_3 films for both thinner Al_2O_3 film thicknesses and thinner Teflon FEP substrate thicknesses. The characterization of cracking density versus compressive stress allowed a quantification of the ability of the alucone interlayer to reduce compressive stress.

II. EXPERIMENTAL SECTION

A. Al_2O_3 ALD and Alucone MLD Film Deposition. The Al_2O_3 ALD and alucone MLD films were grown in a hot-wall, viscous flow reactor similar to reactors that have been described earlier.[8,13,14] The films were deposited at a growth temperature of 135 °C on DuPont Teflon FEP with substrate thicknesses of 50 and 125 μm or HSPEN (DuPont Teijin, Inc.) with a substrate thickness of 25 μm.[15] The reactants were alternately injected into an ultrahigh purity N_2 viscous flow carrier gas traveling through the reactor. The baseline reactor pressure was 600 mTorr with N_2 flowing through the reactor.[8,14]

Al_2O_3 ALD was performed using $Al(CH_3)_3$ (trimethylaluminum (TMA)) and H_2O (water) as the reactants. Al_2O_3 ALD is a model ALD process and is one of the most well-defined ALD systems.[15−17] The two sequential, self-limiting reactions for Al_2O_3 ALD are

$$\text{(A)}\quad AlOH^* + Al(CH_3)_3 \rightarrow AlOAl(CH_3)_2^* + CH_4 \quad (1)$$

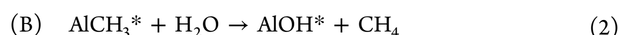

$$\text{(B)}\quad AlCH_3^* + H_2O \rightarrow AlOH^* + CH_4 \quad (2)$$

where the asterisks indicate the surface species. For Al_2O_3 ALD film growth, the substrate is first exposed to TMA. Then after N_2 purging to remove residual reactants and reaction products, the substrate is exposed to water and a second N_2 purging process. This sequence defines one AB cycle for Al_2O_3 ALD. The timing for this sequence was (t_1, t_2, t_3, t_4) where t_1 is the TMA exposure time, t_2 is the N_2 purging time, t_3 is the water exposure time and t_4 is the second N_2 purging time. The timing sequence was (0.8, 75, 0.2, 75) where the times are in seconds. The reactant pressures were both 250 mTorr. The repetition of the AB cycles results in an Al_2O_3 ALD film growth of ~1.2 Å per AB cycle at 135 °C.[14,15,17]

The alucone MLD films were grown using an ABC reactant sequence with TMA, $HOCH_2CH_2OH$ (ethylene glycol (EG)), and H_2O as the reactants. Alucone MLD using TMA and EG in an AB reactant sequence was reported earlier.[18] These alucone films have some remaining $AlCH_3$ species that can react with H_2O and lead to some film instability.[18] The H_2O in the ABC reactant sequence helps to remove the remaining $AlCH_3$ species. For this ABC alucone MLD process, the three sequential, self-limiting reactions are:

$$\text{(A)}\quad AlOH^* + Al(CH_3)_3 \rightarrow AlOAl(CH_3)_2^* + CH_4 \quad (3)$$

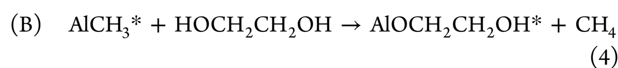

$$\text{(B)}\quad AlCH_3^* + HOCH_2CH_2OH \rightarrow AlOCH_2CH_2OH^* + CH_4 \quad (4)$$

$$\text{(C)}\quad AlCH_3^* + H_2O \rightarrow AlOH^* + CH_4 \quad (5)$$

For alucone MLD film growth, the timing for the ABC alucone MLD reactant sequence was (t_1, t_2, t_3, t_4, t_5, t_6), where t_1 and t_2 are the TMA dosing time and the N_2 purge time following the TMA exposure, t_3 and t_4 are the EG dosing time and the N_2 purge time following the EG exposure, and t_5 and t_6 are the water dosing time and the N_2 purge time following the H_2O exposure. The timing sequence was (0.6, 75, 0.9, 120, 0.2, 120) where the times are in seconds. The repetition of the ABC cycles results in an alucone film growth of ~2 Å per ABC cycle at 135 °C.

B. Measurement of Crack Density from Thermal Compressive Stress. For the measurements of critical compressive strain, the Al_2O_3 ALD films were deposited on Teflon FEP substrates with dimensions of 1 in. × 1 in. at elevated temperature as shown in Figure 1. When the coated substrate cools to room temperature, the Al_2O_3 film is placed under compressive stress because the Teflon contracts more than the Al_2O_3 film.[8] The compressive stress first causes the Al_2O_3 film to buckle during the cooling process as shown in Figure 1b. After additional cooling and more compressive stress, the Al_2O_3 film cracks on the ridge of the buckles as shown in Figure 1c.

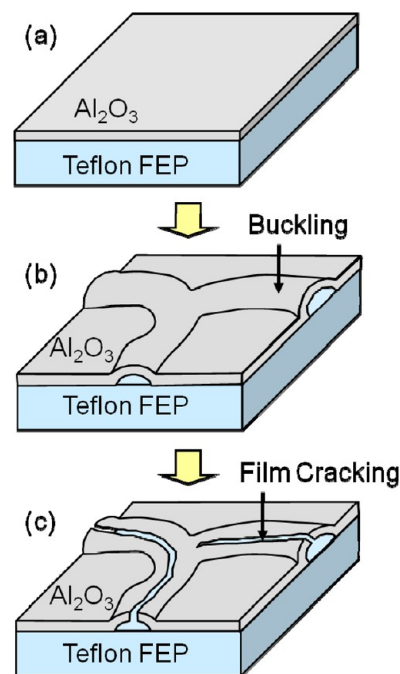

Figure 1. (a) Al_2O_3 ALD film grown at elevated temperature on Teflon FEP substrate. (b) Al_2O_3 film buckles upon cooling from deposition temperature to room temperature. (c) At threshold compressive stress, the Al_2O_3 film cracks.

The magnitude of the compressive stress is defined by the thermal expansion coefficients of Al_2O_3 film and the Teflon FEP substrate. The thermal expansion coefficient of the Al_2O_3 ALD film is 4.2 ppm/K.[19] The thermal expansion coefficient of the Teflon FEP substrate is highly temperature dependent as reported in the literature.[9] The calculation of the compressive stress applied on Al_2O_3 films after growth at different deposition temperatures has been reported previously.[8]

The buckles and crack density in the Al_2O_3 ALD film were analyzed using field-emission scanning electron microscopy (FE-SEM) measurements (JSM-7401F, JEOL).[8] The average crack density and its uncertainty were obtained by analysis of five different FE-SEM images. The crack density was measured for Al_2O_3 films grown directly on the Teflon FEP substrate. The crack density was also measured for Al_2O_3 films grown on alucone interlayers of various thicknesses that were deposited on the Teflon FEP substrate. The measurements explored Al_2O_3 films with thicknesses of 21 and 48 nm. The Teflon FEP substrates had thicknesses of 50 and 125 μm.

C. Calculation of the Thermal Compressive Stress. The thermal stress, σ_f, for a film on an underlying substrate can be calculated simply by the following equation:[8,20]

$$\sigma_f = \frac{E_f}{(1 - \upsilon_f)} \int_{T_1}^{T_2} \{\alpha_s(T) - \alpha_f(T)\} \cdot dT \tag{6}$$

In this equation, E_f is the elastic modulus for the film and ν_f is the Poisson ratio for the film. α_f and α_s are the thermal expansion coefficients for the film and substrate, respectively. This equation yields accurate thermal stresses for the film if the elastic moduli of the film and substrate are comparable.

The elastic modulus of the Al_2O_3 ALD film has been measured as $E = 180$ GPa[21] and $E = 195$ GPa.[19] This elastic modulus is much higher than the elastic modulus of $E = 0.48$ GPa for the Teflon FEP substrate.[22] The higher elastic modulus for the Al_2O_3 ALD film will constrain the shrinkage of the Teflon FEP substrate. The thicker Al_2O_3 film will constrain shrinkage of the Teflon FEP substrate more than the thinner Al_2O_3 film. The thicker Teflon FEP substrate will also be constrained less by the Al_2O_3 film than the thinner Teflon FEP substrate.

As a result of the different elastic moduli for the film and the substrate, a more detailed model is needed to calculate the thermal compressive stress. A model was developed earlier to treat functionally graded material systems. This model presented by Ravichandran can handle different elastic moduli and can also treat different film thicknesses on different substrate thicknesses.[12] The Ravichandran model for the thermal stress will be employed instead of the simple model given by eq 6.

A full description of the Ravichandran model has been given earlier.[12] This study will utilize equations from the Ravichandran model that yield the residual thermal stress, σ_{res}, in the film:[12]

$$\sigma_{res}(y) = E(y)\Delta T\left[\alpha(y) - \frac{A_1}{E_1} - \frac{\left(A_2 - \frac{A_1}{E_1}E_2\right)(yE_1 - E_2)}{(E_1E_3 - E_2^{\,2})}\right] \tag{7}$$

$$A_1 = \int_{-c}^{c} \alpha(y)\, E(y)\, dy \tag{8}$$

$$A_2 = \int_{-c}^{c} \alpha(y)\, E(y) y\, dy \tag{9}$$

$$E_1 = \int_{-c}^{c} E(y)\, dy \tag{10}$$

$$E_2 = \int_{-c}^{c} E(y) y\, dy \tag{11}$$

$$E_3 = \int_{-c}^{c} E(y) y^2\, dy \tag{12}$$

In these equations, the variable y is normal to the surface of the polymer substrate and parallel to the growth direction of the film coatings. The variable c is defined such that the total thickness of the film and substrate is $2c$. y varies from $-c$ to $+c$. $-c$ starts at the bottom of the Teflon FEP substrate. $+c$ ends at the top of the Al_2O_3 ALD film. Given the much larger thickness of the polymer substrate compared with the ALD film coating, the $y = 0$ point is inside the polymer substrate. The thermal expansion coefficient and elastic modulus for each component in the system are given by $\alpha(y)$ and $E(y)$, respectively. The thermal expansion coefficients for the Teflon FEP substrate, alucone interlayer and Al_2O_3 ALD film were 120−170 ppm/K in the temperature range from room temperature to 160 °C,[9] 12 ppm/K[19] and 4.2 ppm/K,[19] respectively. The elastic moduli for the Teflon FEP substrate, alucone interlayer and Al_2O_3 ALD film were 0.48 GPa,[22] 36.8 GPa,[23] and 180 GPa,[23] respectively.

The A_1 and A_2 terms in eqs 8 and 9 yield the symmetric and asymmetric stress of the whole system. E_1 in eq 10 is the symmetrical term of the elastic modulus. E_2 and E_3 in eqs 11 and 12 are the asymmetric terms of the elastic modulus. A positive residual thermal stress is a tensile stress. A negative thermal stress is a compressive stress. Compared with the original equation presented by Ravichandran,[12] note that we have corrected a sign error in front of the third term in the bracketed expession of eq 7.

D. Critical Tensile Strain of Alucone Films on Teflon FEP and HSPEN Substrates. The critical tensile strains of alucone films were measured on Teflon FEP and HSPEN substrates.[8,23] For these measurements, sheets of Teflon FEP and HSPEN were cut into strips with dimensions of 100 mm ×10 mm (gauge section) using a paper cutter. The Teflon FEP and HSPEN strips then were loaded into the reactor for alucone coating. After alucone coating, the Teflon FEP and HSPEN sample strips were cooled to room temperature.

The method to determine the critical tensile strain test was described in detail in a previous recent study.[8] A mechanical tester (Insight 2, MTS Systems Corp.) was used to stress the samples. The tensile strain was applied at the displacement controlled strain rate of 0.015 s^{-1}. The strain was measured with a laser extensometer (LE-05, Electronic Instrument Research Corp.).[8,23] The cracks from strain on the alucone thin film were examined with a confocal microscope (LSM 510, Carl Zeiss, Inc.) with optical visualization using light scattering.

To detect cracks easily with the confocal microscope, the samples were soaked in 0.01N HCl solution for 90 min to etch ~50 nm of alucone film after stressing to a particular tensile strain. The samples were washed with distilled and deionized water to remove the residue HCl solution and then dried using ultrahigh purity N_2 gas. An argon ion laser with the wavelength of 458 nm was then used to examine the cracking of the alucone film. The cracking density was determined from the number of cracks along the direction of the tensile strain over a length of 90 μm.[8] The crack density and uncertainty were averaged for 5 different images.

III. RESULTS AND DISCUSSION

A. Al_2O_3 ALD Film Cracking on Teflon FEP Substrates. A FE-SEM image of Al_2O_3 ALD films that have buckled and cracked on Teflon FEP is shown at low magnification in Figure 2. This image is for an Al_2O_3 film with a thickness of 48 nm.

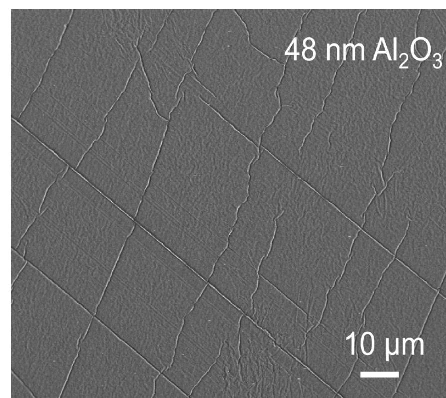

Figure 2. FE-SEM image of an Al_2O_3 ALD film with a thickness 48 nm deposited at 135 °C on a Teflon FEP substrate with a thickness of 125 μm and then cooled to room temperature.

The Al_2O_3 film was deposited at 135 °C on a Teflon FEP substrate with a thickness of 125 μm. The compressive stress on this Al_2O_3 film was 1.58 GPa. This compressive stress was calculated using the Ravichandran model given by eq 7. The FE-SEM image observed in Figure 2 is very similar to the FE-SEM images observed in previous studies of Al_2O_3 ALD film cracking on Teflon FEP.[8] The FE-SEM image of one of the buckles that has cracked is displayed at high magnification in Figure 3.

The crack density in Al_2O_3 ALD films was measured after deposition at different temperatures on Teflon FEP substrates with thicknesses of 50 and 125 μm. The thickness of the Al_2O_3

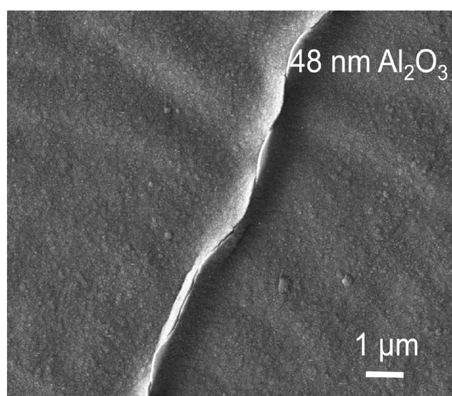

Figure 3. Magnification of section of FE-SEM image in Figure 2 showing cracking at the ridge of one of the buckles in the Al_2O_3 ALD film.

film was 48 nm. Figure 4 shows the cracking density in the Al_2O_3 film on the Teflon FEP substrates versus deposition

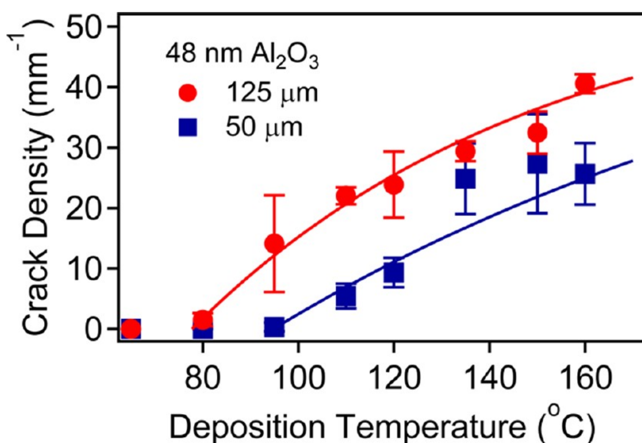

Figure 4. Cracking density versus deposition temperature for Al_2O_3 ALD film with a thickness of 48 nm deposited at different temperatures on Teflon FEP substrates with thicknesses of 50 and 125 μm.

temperature. The solid lines show the fit to an exponential expression with the form $y = y_0\,(1 - \exp[-a(T - T_0)])$ where a is an adjustable parameter.[8] The threshold deposition temperatures, T_0, for cracking are ~78 °C and ~95 °C for the Teflon FEP substrates with thicknesses of 125 and 50 μm, respectively. These different threshold deposition temperatures for different Teflon FEP substrate thicknesses can not be explained using the simple model for thermal stress given by eq 6.

The Ravichandran model for the thermal stress is needed because the deposition temperatures apply different compressive stresses to the Al_2O_3 ALD film depending on the thickness of the Teflon FEP substrate. The thicker Teflon FEP substrate is constrained less by the Al_2O_3 film than the thinner Teflon FEP substrate. Conversely, the thicker Teflon FEP substrate applies larger compressive stress to the Al_2O_3 films. This larger compressive stress leads to a cracking threshold at a lower deposition temperature of ~78 °C for the Teflon FEP substrate with a thickness of 125 μm. Higher deposition temperatures produce higher compressive strains and larger crack densities.

The Ravichandran model given by eq 7 can be used to calculate the residual thermal stress in the Al_2O_3 ALD film after different deposition temperatures on Teflon FEP substrates with thicknesses of 50 and 125 μm. The cracking density versus deposition temperature in Figure 4 can be replotted as cracking density versus compressive stress in Figure 5a. When the

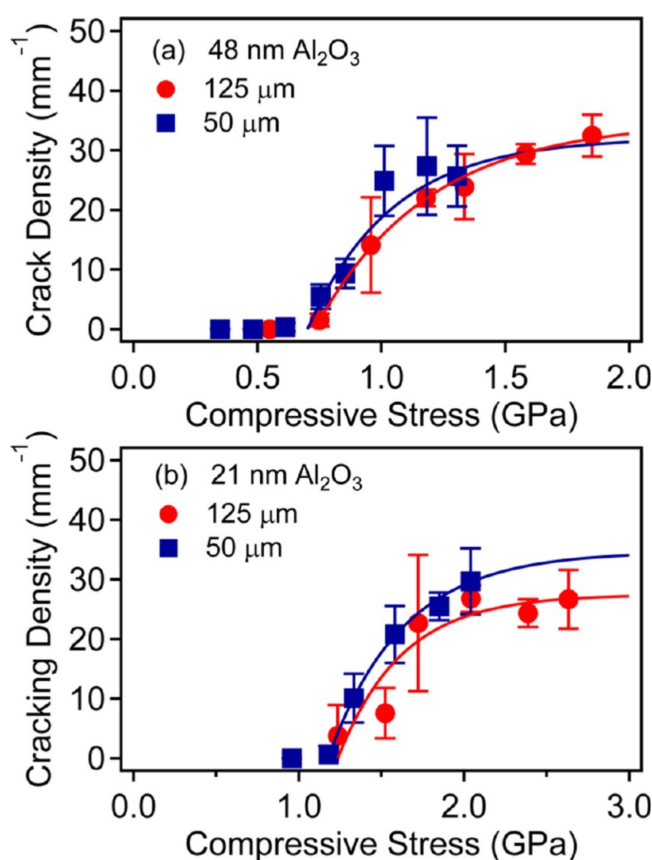

Figure 5. Cracking density versus thermal compressive stress for Al_2O_3 ALD films with thicknesses of (a) 48 nm and (b) 21 nm deposited on Teflon FEP substrates with thicknesses of 50 and 125 μm.

Ravichandran model is employed, the Al_2O_3 film with a thickness of 48 nm is observed to crack at the same critical compressive stress for both Teflon FEP substrate thicknesses of 50 and 125 μm. The identical critical compressive stress for the two Teflon FEP substrate thicknesses argues for the validity of the Ravichandran model.

The solid lines in Figure 5a are based on the exponential fitting form: $y = y_0(1 - \exp[-b(\sigma - \sigma_0)])$.[8] In this expression, y is the crack density, y_0 is the saturation crack density, σ is the compressive stress, σ_0 is the critical compressive stress, and b is an adjustable parameter. The fitting closely approximates the measured crack density versus compressive stress and determines the critical compressive stress, σ_0, when $\sigma - \sigma_0 = 0$. The critical compressive stresses for the Al_2O_3 film with a thickness of 48 nm on Teflon FEP substrates with thicknesses of 50 and 125 μm were 0.74 ± 0.04 GPa and 0.73 ± 0.29 GPa, respectively.

Figure 5b shows the cracking density for Al_2O_3 films with a thickness of 21 nm on Teflon FEP substrates with thicknesses of 50 and 125 μm. The Ravichandran model again predicts the same critical compressive stress for both Teflon FEP substrate thicknesses. The identical critical compressive stress for the two Teflon FEP substrate thicknesses further indicates that the Ravichandran model is correctly accounting for the compres-

sive stress on the Al_2O_3 films. The solid lines based on the exponential form reveal that the critical compressive stresses for the Al_2O_3 film with a thickness of 21 nm on Teflon FEP substrates with thicknesses of 50 and 125 μm, were 1.18 ± 0.09 GPa and 1.16 ± 0.02 GPa, respectively.

Earlier studies measured the critical compressive stresses (strain) of Al_2O_3 ALD films on Teflon FEP substrates.[8] These measurements employed eq 6 to determine the thermal compressive stress (strain). The Ravichandran model can also be employed to determine the thermal compressive stress (strain).[12] The critical compressive stresses (strains) can then be reevaluated for all the Al_2O_3 ALD film thicknesses from 19 to 48 nm. A summary of the critical compressive stresses and strains versus Al_2O_3 film thickness is shown in Figure 6. Compared with the earlier critical compressive stresses (strains), the Ravichandran model yields smaller critical compressive stresses (strains) than determined using eq 6.

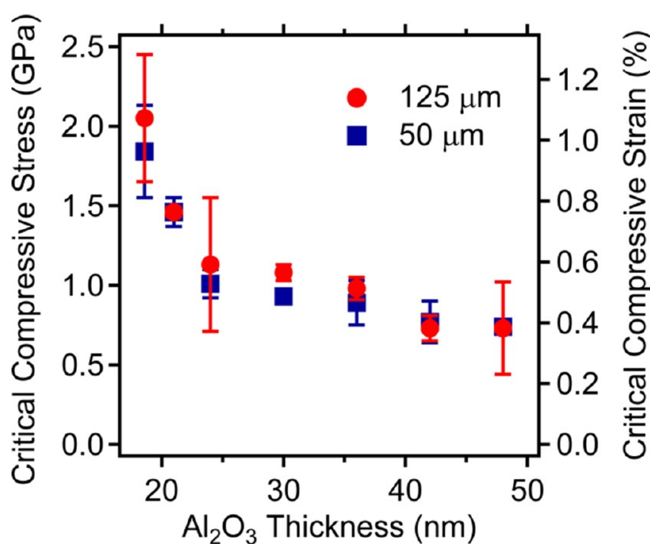

Figure 6. Critical compressive stresses and critical compressive strains for Al_2O_3 ALD films versus film thickness on Teflon FEP substrates with thicknesses of 50 and 125 μm.

B. No Cracking for Alucone Films on Teflon FEP Substrates. Alucone films were used as interlayers to minimize the stress caused by thermal expansion mismatch between the Al_2O_3 ALD films and the Teflon FEP substrates. The alucone interlayer serves as a compensating compliant layer that reduces the stress caused by CTE mismatch. The alucone layer may be ideal as a compensating compliant layer because the alucone film has mechanical properties that are intermediate between Al_2O_3 ALD films and Teflon FEP substrates.

Experiments were first conducted to determine if there was any cracking in the alucone films by themselves on the Teflon FEP substrates. There was no evidence of any cracking or buckling in the alucone films on the Teflon FEP substrates over the entire range of deposition temperatures and compressive stresses. Figure 7 shows FE-SEM images for alucone films deposited at 135 °C and then cooled down to room temperature on Teflon FEP substrates with a thickness of 125 μm. The alucone films with thicknesses of 100 and 200 nm are shown in Figures 7a and 7b, respectively.

The thermal compressive stress applied to the alucone films with a thickness of 100 nm in Figure 7a is calculated to be σ = 0.39 GPa using the Ravichandran model. This calculation used

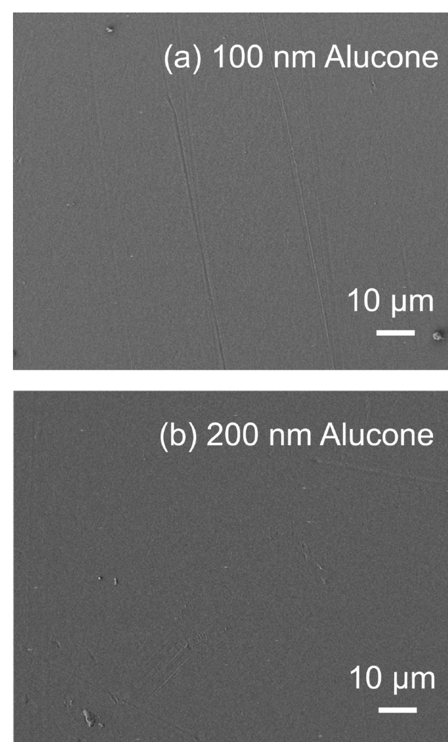

Figure 7. FE-SEM images of alucone films with thicknesses of (a) 100 nm and (b) 200 nm that were deposited at 135 °C on Teflon FEP substrates with a thickness of 125 μm and then cooled to room temperature.

an elastic modulus of E_f = 36.8 GPa and a constant thermal expansion coefficient of α_f = 12 ppm/K for the alucone film.[24] Using the relationship $E = \sigma/\varepsilon$, the compressive stress of σ = 0.39 GPa is equivalent to a compressive strain of ε = −1.06%. For comparison, the thermal compressive stress applied to the alucone film with a thickness of 200 nm in Figure 7b is calculated to be σ = 0.32 GPa using the Ravichandran model.

Alucone films with thicknesses of 20, 40, and 60 nm were also deposited at 135 °C and then cooled to room temperature and examined by FE-SEM. None of the FE-SEM images showed any buckling or cracking. The alucone films with thicknesses of 100 and 200 nm were also deposited at 135 °C and then cooled down to −78 °C using a mixed dry ice and methanol solution. The FE-SEM images of these films also displayed no evidence of any buckling or cracking. The alucone films are able to withstand high compressive strains without cracking.

In contrast to the absence of cracking at high compressive strains, earlier studies revealed that the critical tensile strain of alucone films with a thickness of 100 nm was only ε = 0.69%.[23] This low critical tensile strain was attributed to the lack of cross-linking in the alucone films which enables them to be easily pulled apart.[23] For compressive strains, this lack of cross-linking may be a benefit because the polymer chains in the alucone layer can easily move with respect to each other under compression without cracking.

C. Cracking of Al_2O_3 ALD films on Teflon FEP Substrates with Alucone Interlayers. Alucone interlayers with different thicknesses were deposited between the Al_2O_3 ALD films and the Teflon FEP substrates as shown in Figure 8. The crack density in the Al_2O_3 ALD film was then examined using FE-SEM images. Figure 9 shows the FE-SEM image of an

dx.doi.org/10.1021/am303077x | ACS Appl. Mater. Interfaces 2013, 5, 1165−1173

Figure 8. Schematic of alucone interlayer with variable thickness between an Al_2O_3 ALD film and a Teflon FEP substrate.

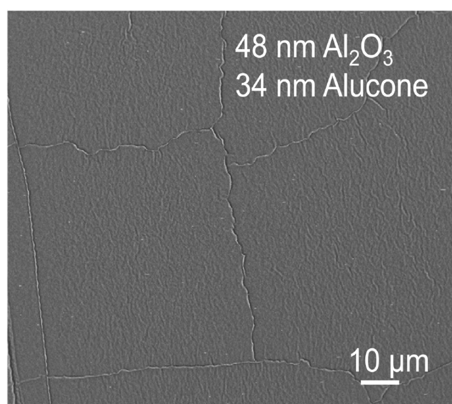

Figure 9. FE-SEM image of an Al_2O_3 ALD film with a thickness of 48 nm on an alucone MLD interlayer with a thickness of 34 nm on a Teflon FEP substrate with a thickness of 125 μm. The ALD and MLD films were deposited at 135 °C and then cooled to room temperature.

Al_2O_3 ALD film with a thickness of 48 nm deposited on an alucone interlayer with a thickness of 34 nm. The Al_2O_3 ALD film and alucone interlayer were both deposited at 135 °C on the Teflon FEP substrate with a thickness of 125 μm. Although cracks are observed in the FE-SEM image in Figure 9, they are greatly reduced compared with the results shown in Figure 2 for the Al_2O_3 ALD film without the alucone interlayer.

Alucone films were able to reduce dramatically the cracking density in the Al_2O_3 ALD films. The reduction of the cracking density was larger for thicker alucone interlayers. Figure 10 shows the cracking density in the Al_2O_3 ALD film with a thickness of 48 nm versus the thickness of the alucone interlayer. The Al_2O_3 ALD films and alucone MLD interlayers were both deposited at 135 °C on the Teflon FEP substrates with thicknesses of 50 and 125 μm. The cracking density is reduced with the increasing thickness of the alucone interlayer. No cracks are measured for alucone interlayer thicknesses of >50 nm on the 50 μm Teflon FEP substrates and >110 nm on the 125 μm Teflon FEP substrates.

The reduction of the cracking density was more dramatic for thinner Al_2O_3 ALD films. Figure 11 shows the cracking density in the Al_2O_3 film with a thickness of 21 nm versus the thickness of the alucone interlayer. The Al_2O_3 films and alucone interlayers were again both deposited at 135 °C on the Teflon FEP substrates with thicknesses of 50 and 125 μm. The cracking density is more rapidly reduced with the thickness of the alucone interlayer. No cracks are measured for alucone interlayer thicknesses of >40 nm on the 50 μm Teflon FEP substrates and >100 nm on the 125 μm Teflon FEP substrates.

The alucone interlayer is able to reduce the stress on the Al_2O_3 ALD film resulting from thermal expansion mismatch with the underlying Teflon FEP substrates. The elimination of cracking in the Al_2O_3 film indicates that the alucone interlayer is able to reduce the compressive stress to below the critical compressive stress of the Al_2O_3 film. Figure 6 shows that

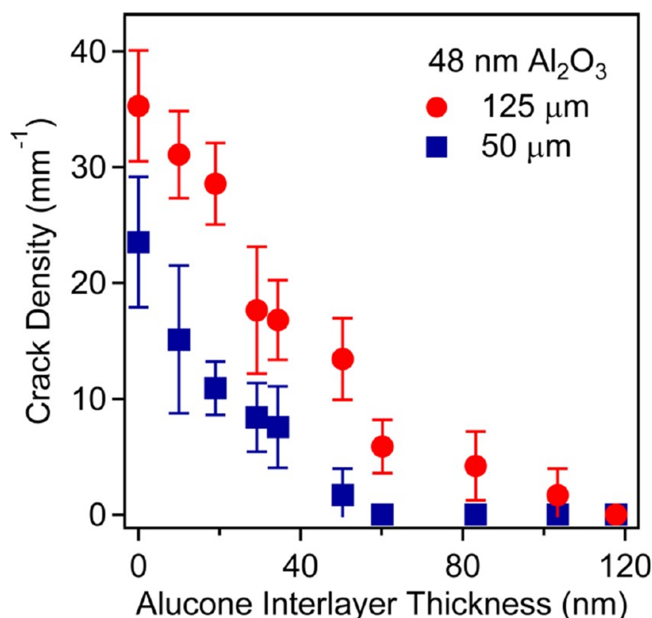

Figure 10. Cracking density of Al_2O_3 ALD films with a thickness of 48 nm deposited on various alucone interlayer thicknesses on Teflon FEP substrates with thicknesses of 50 and 125 μm.

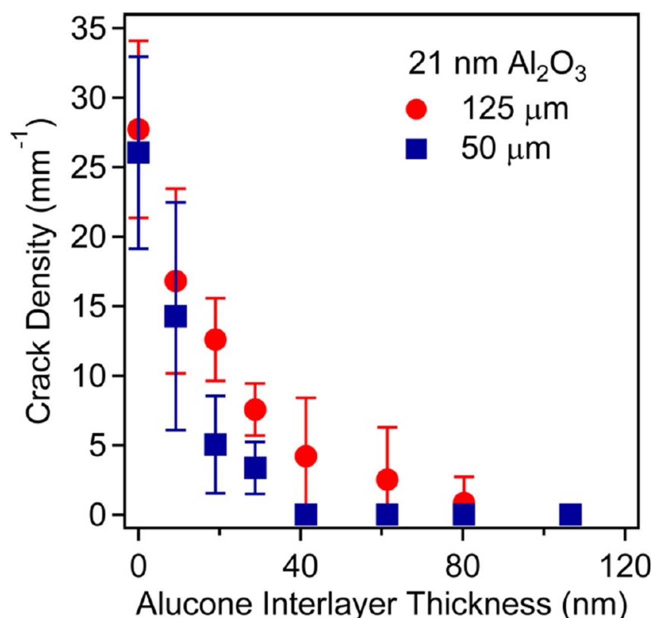

Figure 11. Cracking density of Al_2O_3 ALD films with a thickness of 21 nm deposited on various alucone interlayer thicknesses on Teflon FEP substrates with thicknesses of 50 and 125 μm.

thinner Al_2O_3 ALD films have higher critical compressive stresses.[8] The results in Figures 10 and 11 are consistent with higher critical compressive stresses for the thinner Al_2O_3 ALD films.

D. Understanding the Effect of the Alucone Interlayer. Figures 10 and 11 show that the alucone interlayer reduces the crack density in the Al_2O_3 ALD films with thicknesses of 48 and 21 nm, respectively, that were deposited at 135 °C. The crack densities versus alucone interlayer thickness in Figures 10 and 11 can be compared with the crack densities versus compressive stress in Figure 5 for the same Al_2O_3 ALD film thicknesses *without* the alucone interlayer.

dx.doi.org/10.1021/am303077x | *ACS Appl. Mater. Interfaces* 2013, 5, 1165−1173

Assuming that the measured crack density correlates with a particular compressive stress, compressive stresses can be assigned to the crack densities in Figures 10 and 11 using the measured crack densities versus compressive stress in Figure 5.

For example, Figure 10 indicates that the cracking density is 17.6 mm^{-1} for an Al_2O_3 film with a thickness of 48 nm on an alucone interlayer with the thickness of 29.2 nm on a Teflon FEP substrate with a thickness of 125 μm. Figure 5a indicates that a crack density of 17.6 mm^{-1} occurs at a compressive stress of ~1.06 GPa. This correlation indicates that a compressive stress of ~1.06 GPa must have been present on the Al_2O_3 film with a thickness of 48 nm on the alucone interlayer with a thickness of 29.2 nm on the Teflon FEP substrate with a thickness of 125 μm.

The cracking densities in Figures 10 and 11 can be redefined as corresponding compressive stresses using the crack density versus compressive stress information in Figure 5. Using this correspondence, Figure 12 displays the compressive stress on

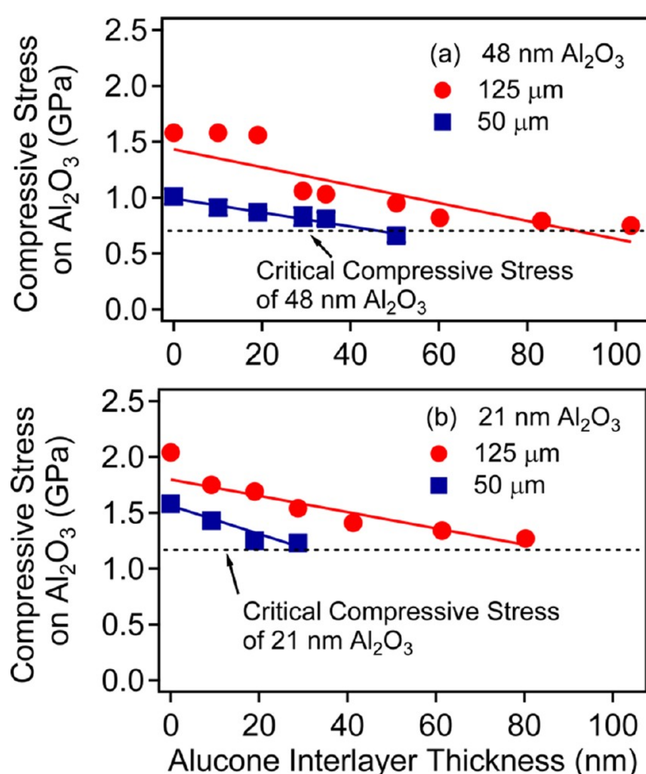

Figure 12. Compressive stress on Al_2O_3 ALD films with thicknesses of (a) 48 nm and (b) 21 nm versus alucone interlayer thickness on Teflon FEP substrates with thickness of 50 and 125 μm. The ALD and MLD films were deposited at 135 °C and then cooled to room temperature.

the Al_2O_3 ALD film versus alucone interlayer thickness. The alucone interlayer progressively reduces the compressive stress on the Al_2O_3 film as a function of alucone interlayer thickness. The dashed lines in Figure 12a and 12b show the critical compressive stresses for the Al_2O_3 films with thicknesses of 21 and 48 nm, respectively. The solid lines in Figure 12 show the linear fitting of the compressive stress versus the alucone interlayer thickness.

This compressive stress reduction versus alucone interlayer thickness can be derived from the linear fits to the data in Figures 12a and 12b. For the Al_2O_3 film with a thickness of 48 nm on Teflon FEP substrates with thicknesses of 50 and 125 μm, the compressive stress reductions were 6.3 MPa/nm and 8.0 MPa/nm, respectively. For the Al_2O_3 film with a thickness of 21 nm on Teflon FEP substrates with thicknesses of 50 and 125 μm, the compressive stress reductions were 12.7 MPa/nm and 7.3 MPa/nm, respectively. The compressive stress reductions are fairly similar for the various Al_2O_3 film thicknesses and Teflon FEP substrate thicknesses. The average compressive stress reduction per thickness of the alucone interlayer is 8.5 ± 2.3 MPa/nm.

Figure 13 shows a pictorial illustration of the reduction of compressive stress on the Al_2O_3 ALD film by the alucone

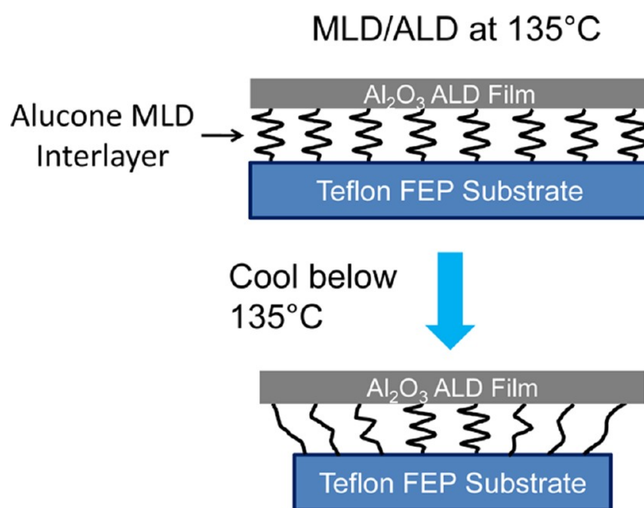

Figure 13. Schematic depicting the “spring-like” nature of the alucone interlayer between the Al_2O_3 ALD film and the Teflon FEP substrate. Upon cooling from 135 °C, the alucone interlayer minimizes the compressive thermal stress on the Al_2O_3 ALD film.

interlayer. The alucone MLD and Al_2O_3 ALD are performed at 135 °C. With cooling from 135 °C to room temperature, the Teflon FEP substrate will contract more than the Al_2O_3 film. This mismatch of thermal expansion coefficients leads to compressive stress on the Al_2O_3 film. However, the “spring-like” alucone interlayer with minimal cross-linking between the polymer chains absorbs some of the compressive stress and lowers the compressive stress applied to the Al_2O_3 film. Consequently, the alucone interlayer is able to protect the Al_2O_3 film from buckling and cracking.

E. Critical Tensile Strain of Alucone Films on Teflon FEP and HSPEN Substrates. The results for the crack density versus tensile strain for alucone films with a thickness of 100 nm deposited on Teflon FEP and HSPEN substrates at 135 °C are shown in Figure 14. The critical tensile strain of the alucone film on the Teflon FEP substrate was much higher than the critical tensile strain for the alucone film with the same thickness on the HSPEN substrate. The critical tensile strains were obtained by fitting the results using an exponential fitting form.[8] Critical tensile strains for the alucone film with a thickness of 100 nm were 1.96 ± 0.12% on Teflon FEP and 0.61 ± 0.12% on HSPEN.

The higher critical tensile strain on the Teflon FEP substrate can be explained by the higher residual compressive stress in the alucone films grown on the Teflon FEP substrates. The compressive stress in the alucone film deposited at 135 °C on the Teflon FEP substrate and then cooled to room temperature

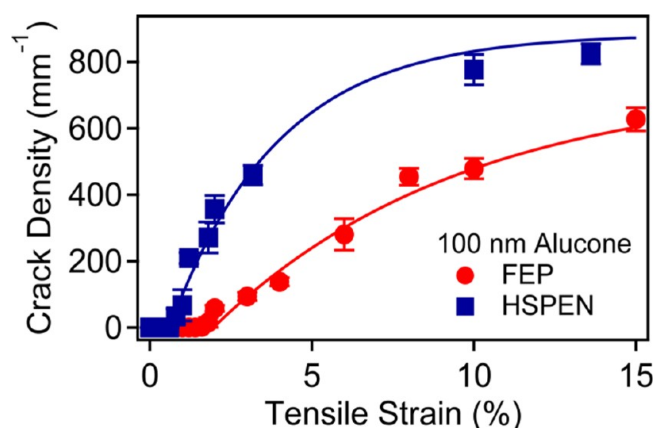

Figure 14. Crack density versus tensile strain for alucone film with a thickness of 100 nm on Teflon FEP and HSPEN substrates. The alucone films were deposited at 135 °C and then cooled to room temperature prior to the application of the tensile strains.

is calculated to be $\sigma = 0.39$ GPa using the Ravichandran model. This compressive stress equates to a compressive strain of $\varepsilon = 1.06\%$ based on an elastic modulus of $E = 36.8$ GPa.[19] This large residue compressive strain can then help offset the applied tensile strain.

The tensile strain applied to the alucone film on Teflon FEP first reduces the residual compressive strain in the alucone film. After removal of the compressive strain, the applied tensile strain leads to a net tensile strain in the alucone film. A critical tensile strain of $\varepsilon = 1.96\%$ is observed for the alucone film on Teflon FEP. This critical tensile strain is close to the residual compressive strain of 1.06% added to the critical tensile strain of 0.61% for cracking of the alucone film on HSPEN. Adding the two strains assumes that the critical tensile strains for alucone films on HSPEN are not affected by residual compressive strains.

The alucone films deposited on HSPEN will have a much smaller residual thermal stress resulting from the thermal expansion coefficient mismatch between the Al_2O_3 ALD film and the HSPEN substrate. Compared with the thermal expansion coefficient of 120−160 ppm/K for Teflon FEP,[9] the HSPEN has a much smaller thermal expansion coefficient of 13 ppm/K.[25] Consequently, the mismatch between the thermal expansion coefficients of the Al_2O_3 ALD film and the HSPEN substrate yields a small residue compressive stress of 5.33 MPa or a compressive strain of only $\varepsilon = 0.014\%$. The compressive stress was calculated using the Ravichandran model after deposition at 135 °C and cooling to 25 °C.

The ability to store residual compressive strain in films may be very useful for films to achieve large critical tensile strains. By using substrates with large thermal expansion coefficients, large thermal compressive stresses can exist in the deposited films after cooling from the deposition temperature. These residual compressive stresses can help offset applied tensile stresses. This strategy may be useful for barrier films deposited on fluoropolymers such as Teflon FEP that have high thermal expansion coefficients. These fluoropolymers are important for thin film solar devices because of their resistance to photodegradation.[7]

IV. CONCLUSIONS

Thermal expansion mismatch between Al_2O_3 ALD films and Teflon FEP substrates was minimized using alucone interlayer films. In the absence of an alucone interlayer, the Al_2O_3 films can crack resulting from the high thermal expansion coefficient mismatch between the Al_2O_3 film and the Teflon FEP substrate. Cracks were observed by FE-SEM images of Al_2O_3 ALD films with thicknesses of 48 and 21 nm grown directly on Teflon FEP substrates with thicknesses of 50 and 125 μm at temperatures from 100 to 160 °C and then cooled to room temperature. The Ravichandran model for residual compressive stress was used to analyze the results and obtain the correlation between crack density and thermal compressive stress.

Under identical conditions using an alucone interlayer, the Al_2O_3 ALD film had a crack density that was reduced progressively versus alucone interlayer thickness. For Al_2O_3 film thicknesses of 48 nm deposited at 135 °C, no cracks were observed for alucone interlayer thicknesses >60 nm on 50 μm thick Teflon FEP substrates. For thinner Al_2O_3 film thicknesses of 21 nm deposited at 135 °C, no cracks were observed for alucone interlayer thicknesses >40 nm on 50 μm thick Teflon FEP substrates. Slightly higher alucone interlayer thicknesses are required to prevent cracking on thicker Teflon FEP substrates with a thickness of 125 μm.

The crack density versus alucone interlayer thickness for Al_2O_3 ALD films grown on alucone interlayers on Teflon FEP was compared with the crack density versus compressive stress for Al_2O_3 ALD films grown directly on Teflon FEP. This comparison revealed that the alucone interlayer thickness linearly reduced the compressive stress on the Al_2O_3 films. The compressive stress reduction per thickness of the alucone interlayer was determined to be ∼8.5 MPa/nm. Comparison of the critical tensile strains for alucone films on Teflon FEP and HSPEN substrates demonstrated that residual compressive stress can help offset applied tensile stress and produce much higher critical tensile strains.

AUTHOR INFORMATION

Corresponding Author

*E-mail: steven.george@colorado.edu.

Notes

The authors declare no competing financial interest.

ACKNOWLEDGMENTS

This work was funded by the DuPont Central Research and Development and the Air Force Office of Scientific Research. We also acknowledge the Nanomaterials Characterization Facility (NCF) at the University of Colorado for the FE-SEM measurements. We also thank Prof. Qi from the Dept. of Mechanical Engineering at the University of Colorado for help with the laser extensometer for the tensile strain experiments.

REFERENCES

(1) Carcia, P. F.; McLean, R. S.; Groner, M. D.; Dameron, A. A.; George, S. M. *J. Appl. Phys.* **2009**, *106*, 023533.
(2) Carcia, P. F.; McLean, R. S.; Reilly, M. H.; Groner, M. D.; George, S. M. *Appl. Phys. Lett.* **2006**, *89*, 031915.
(3) Groner, M. D.; George, S. M.; McLean, R. S.; Carcia, P. F. *Appl. Phys. Lett.* **2006**, *88*, 051907.
(4) Chen, T. N.; Wuu, D. S.; Wu, C. C.; Chiang, C. C.; Chen, Y. P.; Horng, R. H. *Plasma Processes Polym.* **2007**, *4*, 180.
(5) Cros, S.; de Bettignies, R.; Berson, S.; Bailly, S.; Maisse, P.; Lemaitre, N.; Guillerez, S. *Sol. Energy Mater. Sol. Cells* **2011**, *95*, S65.
(6) Lewis, J. S.; Weaver, M. S. *IEEE J. Sel. Top. Quantum Electron.* **2004**, *10*, 45.
(7) DeBergalis, M. *J. Fluorine Chem.* **2004**, *125*, 1255.

(8) Jen, S. H.; Bertrand, J. A.; George, S. M. *J. Appl. Phys.* **2011**, *109*, 084305.
(9) Kirby, R. K. *J. Res. Nat. Bur. Stand.* **1956**, *57*, 91.
(10) Korner, L.; Sonnenfeld, A.; Heuberger, R.; Waller, J. H.; Leterrier, Y.; Manson, J. A. E.; von Rohr, P. R. *J. Phys. D: Appl. Phys.* **2010**, *43*, 115301.
(11) Cho, J. R.; Ha, D. Y. *Mater. Sci. Eng., A* **2002**, *334*, 147.
(12) Ravichandran, K. S. *Mater. Sci. Eng., A* **1995**, *201*, 269.
(13) Dameron, A. A.; Davidson, S. D.; Burton, B. B.; Carcia, P. F.; McLean, R. S.; George, S. M. *J. Phys. Chem. C* **2008**, *112*, 4573.
(14) Elam, J. W.; Groner, M. D.; George, S. M. *Rev. Sci. Instrum.* **2002**, *73*, 2981.
(15) Groner, M. D.; Fabreguette, F. H.; Elam, J. W.; George, S. M. *Chem. Mater.* **2004**, *16*, 639.
(16) Dillon, A. C.; Ott, A. W.; Way, J. D.; George, S. M. *Surf. Sci.* **1995**, *322*, 230.
(17) Ott, A. W.; Klaus, J. W.; Johnson, J. M.; George, S. M. *Thin Solid Films* **1997**, *292*, 135.
(18) Dameron, A. A.; Seghete, D.; Burton, B. B.; Davidson, S. D.; Cavanagh, A. S.; Bertrand, J. A.; George, S. M. *Chem. Mater.* **2008**, *20*, 3315.
(19) Miller, D. C.; Foster, R. R.; Jen, S. H.; Bertrand, J. A.; Cunningham, S. J.; Morris, A. S.; Lee, Y. C.; George, S. M.; Dunn, M. L. *Sens. Actuators, A* **2010**, *164*, 58.
(20) Leterrier, Y. *Prog. Mater. Sci.* **2003**, *48*, 1.
(21) Tripp, M. K.; Stampfer, C.; Miller, D. C.; Helbling, T.; Hermann, C. F.; Hierold, C.; Gall, K.; George, S. M.; Bright, V. M. *Sens. Actuators, A* **2006**, *130*, 419.
(22) *DuPont FEP Fluorocarbon Film Properties Bulletin*; DuPont Fluroproducts: Wilmington, DE, 2010.
(23) Miller, D. C.; Foster, R. R.; Zhang, Y. D.; Jen, S. H.; Bertrand, J. A.; Lu, Z. X.; Seghete, D.; O'Patchen, J. L.; Yang, R. G.; Lee, Y. C.; George, S. M.; Dunn, M. L. *J. Appl. Phys.* **2009**, *105*, 093527.
(24) Miller, D. C.; Foster, R. R.; Jen, S. H.; Bertrand, J. A.; Seghete, D.; Yoon, B.; Lee, Y. C.; George, S. M.; Dunn, M. L. *Acta Mater.* **2009**, *57*, 5083.
(25) MacDonald, W. A.; Looney, M. K.; MacKerron, D.; Eveson, R.; Adam, R.; Hashimoto, K.; Rakos, K. *J. Soc. Inf. Disp.* **2007**, *15*, 1075.